PHYSICAL REVIEW C **81**, 054314 (2010)

Bound, virtual, and resonance *S*-matrix poles from the Schrödinger equation

A. M. Mukhamedzhanov,[1] B. F. Irgaziev,[2] V. Z. Goldberg,[1] Yu. V. Orlov,[3] and I. Qazi[2]
[1]*Cyclotron Institute, Texas A&M University, College Station, Texas 77843, USA*
[2]*GIK Institute of Engineering Sciences and Technology, Topi, Pakistan*
[3]*Institute of Nuclear Physics, Moscow State University, Moscow, Russia*

(Received 21 May 2009; revised manuscript received 19 April 2010; published 20 May 2010)

A general method, which we call the potential *S*-matrix pole method, is developed for obtaining the *S*-matrix pole parameters for bound, virtual, and resonant states based on numerical solutions of the Schrödinger equation. This method is well known for bound states. In this work we generalize it for resonant and virtual states, although the corresponding solutions increase exponentially when $r \to \infty$. Concrete calculations are performed for the 1^+ ground state of ^{14}N, the resonance ^{15}F states ($1/2^+, 5/2^+$), low-lying states of ^{11}Be and ^{11}N, and the subthreshold resonance in the proton-proton system. We also demonstrate that in the case of broad resonances, their energy and width can be found from the fitting the experimental phase shifts using the analytical expression for the elastic-scattering *S* matrix. We compare the *S*-matrix pole and the *R* matrix methods for broad resonances in the ^{14}O-p and in ^{26}Mg-n systems.

DOI: 10.1103/PhysRevC.81.054314 PACS number(s): 24.50.+g, 25.70.Ef, 25.70.Hi, 27.20.+n

I. INTRODUCTION

Analysis of the *S*-matrix pole structure is a powerful method in quantum physics. It is well known that the poles of the *S* matrix in the complex momentum (or energy) plane correspond to bound, virtual, and resonance states. There is a well-known relation between the *S* matrix and Jost functions, the singular solutions of the Schrödinger equation at $r \to 0$. The conventional numerical method for bound states is to search for solutions, which only have an outgoing wave at pure imaginary momenta in the upper half momentum plane. The corresponding wave function is an exponentially decreasing solution when $r \to \infty$.

Virtual or resonance states are described by the wave functions containing only the outgoing waves asymptotically, which exponentially increase due to the complex momenta. In the past (see Ref. [1] and references therein), the analytical continuation onto the unphysical energy sheet of the Lippmann-Schwinger as well as the momentum-space Faddeev integral equations were used to find the resonance properties. The normalization formula for the bound state vertex function in the momentum space was generalized in Ref. [2] for the resonance and virtual states.

Such states are considered as unaccomplished bound states. This means that a bound state pole should move down the positive semiaxis of the complex momentum plane while the interaction strength decreases. At some critical value of the interaction strength, the pole approaches the zero energy point, which belongs to the contour of integration. After a subsequent decrease of the interaction strength, the pole moves to the lower part of the complex momentum plane (unphysical energy sheet) dragging the integration contour in the Lippmann-Schwinger equation to secure the convergence of the integral. This leads to the appearance of an extra term in the right-hand side of the equation, which is the residue of the integrand at the pole.

This method of the analytical continuation has been applied successfully to different physical systems. Unfortunately, it cannot be used directly in the case of charged particles. We should also note that an analytical form of the Fourier transform of the potential, which is an input in the Lippmann-Schwinger integral equations, is known only for a limited number of potentials.

The problem of the exponential increase of the Gamow resonance wave function in the asymptotic region can be solved by a complex scaling method based on the so-called ABC theorem [3]. This method consists of solving the Schrödinger equation on a ray in the first quadrant of the radial complex plane rather than on the real axis of the coordinate *r*. This ray can be obtained by the following transformation of the radial coordinate *r* and the conjugate momentum *p*: $r \to r\,\exp(i\theta)$ and $p \to p\,\exp(-i\theta)$. As a result, the bound state spectrum is supplemented by the *S*-matrix poles situated in the sector defined by the angle θ between the real axis and the ray in the fourth quadrant of the complex momentum plane. The axis rotation angle, θ, is limited by the position of the potential singularities in the radial complex plane. It is important that the complex scaling method can be applied to the case of charged particles. The method is valid if the Coulomb potential satisfies the scaling condition of the ABC theorem. This is true only for the pointlike Coulomb, which behaves like $1/r$ or for the Coulomb potential of a diffuse sphere. An application of this method to resonances in nuclear reactions was presented in Ref. [4]. The numerical realization of this method is a rather complex one.

A few different techniques to determine the resonance energy, width, and resonance wave function based on the solution of the Schrödinger equation have been previously suggested. Instead of the Zel'dovich's normalization procedure [5], which is difficult in practical realization due to slow convergence of the integrals, in these methods the normalization of the resonant wave function is achieved using the rotation of the integration countour over *r* from $R_{\max}$ to the complex plane, where the nuclear potential is cut to zero. First we refer to the method of solution of the radial Schroödinger equation to determine resonances suggested in

Ref. [6] (GAMOW code). The method is designed to find poles corresponding to resonances, subthreshold resonances, and virtual states. In this method the complex eigenvalue and the Gamow wave function can be found by integration of the Schrödinger equation imposing the boundary conditions in the origin and the asymptotic region. To solve the equation the Fox-Goodwin numerical method with fixed step length was applied and the logarithmic derivatives of the internal and external wave functions were matched. In Ref. [7] the GAMOW code was used to determine the antibound poles. An improved version of the the GAMOW code, which uses the piecewise perturbation method for integration of the radial equation numerically, has been presented in Ref. [8] (code ANTI), which was designed to determine the virtual states, virtual resonances, and the broad resonance by introducing complex Woods-Saxon potential. In Ref. [9] the virtual states were calculated using the Berggren representation. In Ref. [10] the Berggren basis was used to calculate the isobaric analog states.

The GAMOW code uses potentials with the finite interaction radius because of the problem with numerical calculation of the exponentially increasing wave function. In Ref. [11] the dependence of the resonance pole found using the GAMOW code on the cut-off radius $R_{\max}$ of the Woods-Saxon potential was discussed for neutron case and for very broad resonances. The reason for such dependence is due to the fact that cutting the Woods-Saxon potential at different distances represent different potentials. The application of the method [6] for the unstable nuclei can be found in Refs. [12,13].

A pole search has also been used in Ref. [14] by solution of the Schrödinger equation with the short-range interaction for the scattering wave function. The norm of the Gamow resonant wave functions does exists for charged particles also [15,16]. The method allows one to find resonances and even subthreshold resonances but it cannot be applied to the virtual states.

The method, which is also close to our approach, was discussed in Ref. [17]. The asymptotic wave function in this method contains the auxiliary $\tilde{S}$ matrix that coincides with the physical S matrix at the resonance poles at which the solution becomes a pure outgoing wave. The method was applied for determination of the low-energy ^{5}He and ^{5}Li resonance parameters [17]. The importance of the pole search has been addressed in the recent review [18].

In the present work, we demonstrate how to find the poles of the S matrix corresponding to bound, virtual, and resonance states and the S-matrix residues in these poles by solving the Schrödinger equation with the nuclear plus Coulomb potentials using the analytical properties of the S matrix. For numerical solution we use the MATHEMATICA package which allows us to find the exact values of the outgoing and incoming Coulomb waves almost from near the origin up to the asymptotic distances both for real and complex values for wide interval of the Coulomb parameter. In contrast to the previously published methods, in our S-matrix pole method the normalization of the resonant wave function is based on the connection between the residue of the S matrix in the pole and the asymptotic normalization coefficient (ANC). This relationship is universal and can be applied to bound, virtual, and resonance (narrow and broad) states [16], making our technique universal, and that is the main distinction of our method from the previously published ones. The ANC is the amplitude of the tail of the bound, virtual, or resonant normalized wave function [16,19]. For the resonant state, the ANC is related to the resonance width [16]. The use of the ANC does not require the normalization of the state corresponding to the S-matrix pole and this why our method allows one to determine both narrow and broad resonances and even antibound states.

A simple relation between the ANC (nuclear vertex constant) and the overall normalization of the peripheral astrophysical S factor suggested in Refs. [20–22] makes it extremely important for obtaining astrophysical S factors. Note that the normalization method proposed by Zel'dovich [5] was generalized in Ref. [16] for the interaction potential with a Coulomb tail.

The S-matrix pole method addressed here has been applied earlier to the virtual (singlet) deuteron and virtual triton with different short-range potentials. The results of the two-step Gamov-state normalization for the virtual (antibound) state of ^{3}H were published in Ref. [23]. For charged particles, the virtual state becomes a subthreshold resonance [24]. Here we present new results for the subthreshold resonance for the ground state of ^{2}He. We also calculate the ground state of ^{14}N and the resonance states of ^{15}F. Finally, our method is applied to the three lowest $T = \frac{3}{2}$ states in ^{11}Be and ^{11}N. Considering the $\frac{1}{2}^+$ state in ^{11}N as an example, we demonstrate how to determine in a model-independent way the energy and width of the broad resonance using the S-matrix analytical structure, which includes the resonant pole. Moreover, we demonstrate that the potential S-matrix pole method addressed here gives the resonance energy and width, which are very close to the model-independent results obtained from the analytical expression for the S matrix in the vicinity of a single pole [25].

We use the system of units in which $\hbar = c = 1$.

II. A NUMERICAL CALCULATION METHOD

To describe the nuclear interaction for the nucleus $A + N$, $N = n, p$ we adopt the Woods-Saxon potential

$$V_N(r) = -V_0 \frac{1}{1+\exp[(r-R)/a]} + V_{ls}(\mathbf{l}\cdot\mathbf{s}) \frac{2}{m_\pi^2} \frac{d}{r\,dr} \left\{ \frac{1}{1+\exp[(r-R_{ls})/a_{ls}]} \right\}, \quad (1)$$

where V_0 (V_{ls}) is the depth of the central (spin-orbital) potential, $\mathbf{l}$ is the orbital momentum operator for the relative motion of A and N, $\mathbf{s}$ is the spin operator of the nucleon, m_π is the pion mass, $R = r_0\, A^{1/3}$, r_0 is the radius parameter of the central nuclear potential and a is its diffuseness, $R_{ls} = r_{ls}\, A^{1/3}$ is the radius of the spin-orbital potential, r_{ls} and a_{ls} are the radius and diffuseness of the spin-orbital potential, A is the atomic mass number of the core. The Coulomb interaction potential is taken in the form

$$V_C(r) = \begin{cases} \frac{Z_1 Z_2 e^2}{2R_C}\left(3 - \frac{r^2}{R_C^2}\right), & r \leqslant R_C, \\ \frac{Z_1 Z_2 e^2}{r}, & r > R_C, \end{cases} \tag{2}$$

where $Z_1 e$ and $Z_2 e$ are the charges of the particles; $R_C = r_C\, A^{1/3}$ (r_C is the parameter of the Coulomb radius).

The radial wave function $u_l(r)$ for the partial wave with the orbital momentum l is the solution of the radial Schrödinger equation (μ_{12} is the reduced mass, E is the energy in the center-of-mass system)

$$\left\{\frac{d^2}{dr^2} + 2\mu_{12}[E - V(r)] - \frac{l(l+1)}{r^2}\right\} u_l(r) = 0. \tag{3}$$

Here, $u_l(r)$ satisfies the standard boundary condition at the origin:

$$u_l(r)|_{r=0} = 0. \tag{4}$$

To write the boundary condition for the derivative of $u_l(r)$, we analyze the behavior of the wave function near the origin. The sum of the potentials $V(r) = V_N(r) + V_C(r)$ multiplied by r is limited. Therefore we choose the point r_0 near the origin and denote $k_0^2 = 2\mu_{12}[E - V(r_0)]$.

The solution of the Schrödinger equation

$$\left\{\frac{d^2}{dr^2} + k_0^2 - \frac{l(l+1)}{r^2}\right\} u_l(r) = 0, \tag{5}$$

which satisfies the condition (4), is proportional to the function $g_l(k_0 r) = k_0 r \cdot j_l(k_0 r)$, where $j_l(k_0 r)$ is the spherical Bessel function. Taking this into account, one can use the initial condition for Eq. (3) as follows

$$u_l(r)|_{r=r_0} = g_l(k_0 r_0), \quad u_l'(r)|_{r=r_0} = k_0 g_l'(k_0 r_0). \tag{6}$$

Note that the energy E is negative for bound and virtual states and complex for resonance states. In the external region $r > R_0$, where the nuclear potential can be omitted with reasonable accuracy, the general solution of Eq. (3) is given by

$$u_l(r) \cong u_l^{as}(r) = C_l^{(-)}(k) u_l^{(-)}(kr) - C_l^{(+)}(k) u_l^{(+)}(kr), \tag{7}$$

where $k = \sqrt{2\mu_{12}E}$, $C_l^{(\pm)}$ are the coefficients that can be found by matching $u_l(r)$ to the solution in the internal region at $r = R_0$.[1] The functions $u_l^{(\pm)}(\rho)$ can be written in terms of the regular $F_l(\eta, \rho)$ and the irregular $G_l(\eta, \rho)$ Coulomb wave functions

$$u_l^{(\pm)}(\rho) = e^{\mp \delta_l^C}[G_l(\eta, \rho) \pm i F_l(\eta, \rho)], \tag{8}$$

where $\eta = Z_1 Z_2 e^2 \mu_{12}/k$ is the Sommerfeld parameter, δ_l^C is the Coulomb phase shift given by $\delta_l^C = \arg\Gamma(1 + l + i\eta)$ and $\rho = kr$. The asymptotic forms of $u_l^{(\pm)}(\rho)$ are given by

$$u_l^{(+)}(\rho) \to \exp\left[i\left(\rho - \eta \ln 2\rho - \frac{l\pi}{2}\right)\right], \quad \rho \to \infty, \tag{9}$$

$$u_l^{(-)}(\rho) \to \exp\left[-i\left(\rho - \eta \ln 2\rho - \frac{l\pi}{2}\right)\right], \quad \rho \to \infty. \tag{10}$$

The coefficients $C_l^{(+)}(k)$ and $C_l^{(-)}(k)$ are proportional to the corresponding Jost functions [26,27]. The functions $u_l^{(+)}$ and $u_l^{(-)}$ are the singular (at the origin) solutions of the Shrödinger equation describing the outgoing and incoming waves, correspondingly. We match the regular solution $u_l(r)$ of the Schrödinger equation (3) with the nuclear and Coulomb potentials to the asymptotic solution (7) at asymptotic radius R_0 in contrast to the asymptotic series of the Coulomb functions in the GAMOW code [6]. Therefore, the value of R_0 is much smaller than $R_{\max}$ in Ref. [6]. We can solve the Schrödinger equation numerically and search for the energy at which the coefficient $C_l^{(-)}(k)$ vanishes. This condition $[C_l^{(-)}(k) = 0]$ means that we are dealing with only the outgoing wave in the asymptotic region ($r \to \infty$). Note that for virtual and resonance states the first term in Eq. (7) is much smaller than the second one, which makes it difficult to obtain a solution and an eigenvalue. To make sure that $C_l^{(-)}(k)/C_l^{(+)}(k)$ goes to zero, we calculate the ratio of the Schrödinger equation solution (for the sum of a nuclear and the Coulomb potentials) and the outgoing wave in the Coulomb potential. This ratio must approach a constant in the asymptotic region. We also check the equality of the logarithmic derivatives of $u_l(r)$ and $u_l^{(+)}(kr)$ at $r = R_0$. R_0 should be chosen larger than the radius of the nuclear potential. According to the scattering theory [27], the vanishing of $C_l^{(-)}$ at the positive imaginary semiaxis in the complex momentum plane corresponds to the bound state, while that on the negative imaginary semiaxis corresponds to the virtual (antibound) state. The resonant state is defined by the zero of $C_l^{(-)}$ in the fourth quadrant of the complex momentum plane.

The S matrix is the ratio $C_l^{(+)}(k)/C_l^{(-)}(k)$, which has a pole at $k = k_0$ if $C_l^{(-)}(k_0) = 0$ [26]. For the poles of S matrix of the first order the residue at the pole k_0 should be

$$\text{Res}\,[S_l(k_0)] = A_l(k_0) = \frac{C_l^{(+)}(k_0)}{C_l^{(-)\prime}(k_0)}, \tag{11}$$

where $C_l^{(-)\prime}(k_0)$ is the derivative at the pole $k = k_0$. To find $A_l(k_0)$, we calculate $C_l^{(-)}(k)$ close enough to the pole k_0. Then, we use the fit function

$$C_l^{(-)}(k) = a_1(k - k_0) + a_2(k - k_0)^2 \tag{12}$$

to obtain the coefficients of the expansion a_1 and a_2 for which $C_l^{(-)\prime}(k_0) = a_1$. The described method we call the potential S-matrix pole method.

---

[1] Note that in contrast to the asymptotic wave function used in Ref. [6] our asymptotic function (7) contains both outgoing wave and incoming wave.

III. RESULTS

A. The ground state of ^{14}N

To show how the method works, we start from *instructive* application to the ground state of ^{14}N considering it as a two-body bound state $^{14}\text{N} = {}^{13}\text{C} + p$. We assume that the proton in the $1p_{1/2}$ orbital is coupled to the $1/2^-$ ground state of ^{13}C to form the 1^+ ground state of ^{14}N.

To describe these states in the two-body (core+nucleon) approach, we choose the geometrical parameters of the bound state Woods-Saxon potential to be $r_0 = r_C = 1.2$ fm and $a = 0.5$ fm. The well-depth procedure providing the experimental binding energy leads to $V_0 = 51.445$ MeV and $V_{ls} = 1.5$ MeV. The coefficients $C_l^{(+)}(k)$ and $C_l^{(-)}(k)$ are found from the set of equations $u_l(r_1) = u_l^{as}(r_1), u_l(r_2) = u_l^{as}(r_2)$ (u_l^{as} is the known asymptotic solution), where both the neighboring points r_1 and r_2 should be chosen in the asymptotic region. In this work we choose as an example $r_1 = 0.5R_{\max}$ and $r_2 = 0.501R_{\max}$, where $R_{\max} = NR$. The parameter N should be big enough to fulfill the condition $u_l(r_1)/u_l^{as}(r_1) = \text{const}$. In Figs. 1 and 2, the wave function for the 1^+ state of ^{14}N and the ratio of the wave function to the Whittaker function describing its asymptotic behavior are shown. From these figures, one can conclude that the coefficient $C_l^{(-)}(k)$ is equal to zero and the wave function coincides with its asymptotic form when $r > R_0$.

From Eq. (7) we get that in the external region the radial bound-state wave function is given by

$$u_l^{(bs)as}(r) = C_l^{(+)}(k)u_l^{(+)}(kr), \tag{13}$$

where $k = i\kappa_{bs}$ ($\kappa_{bs} > 0$). Normalizing the bound-state wave function to unity we can rewrite its asymptotic term as

$$u_l^{(bs)as}(r) = b_l\, W_{-\eta_{bs},l+1/2}(2\,\kappa_{bs}\, r), \tag{14}$$

where b_l is the single-particle ANC, $W_{-\eta_{bs},l+1/2}(2\,\kappa_{bs}\, r)$ is the Whittaker function determining the radial shape of the bound-state wave function, η_{bs} is the Coulomb parameter for the bound state, $\kappa_{bs} = \sqrt{2\,\mu_{12}\varepsilon_{bs}}$ is the bound-state wave number, and ε_{bs} is the binding energy of the bound state. For the adopted geometrical parameters, we get $b_{1(gr)} = 4.289$ fm$^{-1/2}$. Note that the single-particle ANC is sensitive to these parameters [28].

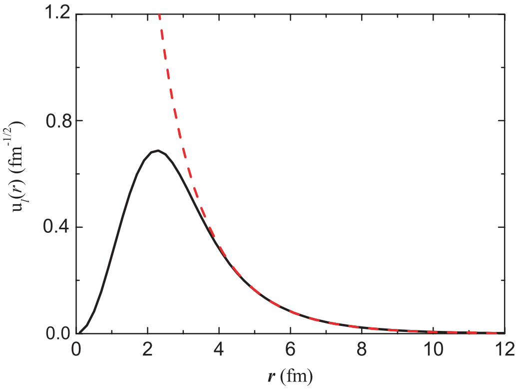

FIG. 1. (Color online) Comparison of the normalized radial bound state wave function for the ^{14}N (1^+) state (solid line) with the corresponding asymptotic form [$W_{-\eta,l+1/2}(2\kappa r)$, dashed line].

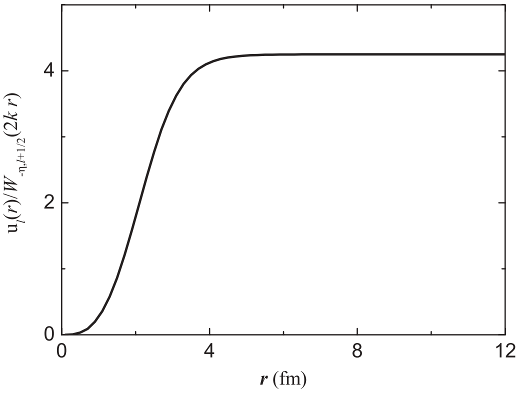

FIG. 2. Ratio of the calculated radial bound state wave function to the Whittaker function ($W_{-\eta,l+1/2}(2\kappa r)$) for the ^{14}N ($1^+$) state.

The residue at the bound state pole of the S matrix is given by [25]

$$A_l(k_0) = (-1)^{l+1} i\, b_l^2. \tag{15}$$

Our calculated residue of the S matrix at pole related to the ground state give the values $A_{gr} = 18.400\,i$ fm^{-1}. Found from this residue, the single-particle ANC coincide with $b_{1(gr)}$ given above and found from the bound-state wave function. This validates the method of calculation of the residue of the S matrix at the bound-state pole presented here.

B. Virtual (antibound) state

Here we apply our method to obtain the energy of the virtual (antibound) state in the $n\,p$ system at $l = 0$, taking into account only the short-range Yukawa nuclear potential $V_N(r) = V_0\, r^{-1}\, \exp(-r/R)$. The virtual state corresponds to $k = -i\,\kappa$ ($\kappa > 0$), i.e., the pole of the S-matrix is located on the negative imaginary semi-axis in the complex momentum plane. It generates the exponentially increasing term $u_0^{(+)}(kr)$ when $r \to \infty$ while the second term $u_0^{(-)}(kr)$ becomes exponentially small making it very difficult to determine the energy (momentum) when $C_0^{(-)} = 0$, which is the condition for the virtual pole. For this reason, to calculate $C_0^{(-)}(-i\kappa)$, one should obtain a solution with very high precision. In our calculations, the energy $|\epsilon_v(N)|$ of the virtual state calculated as function of $R_{\max} = N\,R$ decreases smoothly as N increases. However, when $N > N_{\max}$ the energy exhibits a sudden change to the larger value. It means that for $r \geqslant R_{\max}$ the solution is not precise enough to calculate $C_0^{(-)}(-i\kappa)$ accurately. That is why we adopt $\epsilon_{np} = \epsilon_v(N_{\max})$ as the virtual pole energy. Our result $\epsilon_{np} = -0.067$ MeV agrees very well with the one obtained using the integral equation method [1,29]. The calculated residue of S-matrix in pole is $A_{np} = -0.072i$ fm^{-1} leading to the single-particle ANC for the virtual $n\,p$ state $b_0 = 0.268$ fm$^{-1/2}$.

C. The resonance states of ^{15}F($1/2^+$, $5/2^+$)

Several articles were published recently [30–34] testing the predictive power of the current theoretical approaches to describe the lowest broad levels in ^{15}F. The final goal of these analyses was a comparison of the predictions with the available experimental data on the ^{15}F levels. Determination of a broad resonance parameters is a well-known unsolved problem in physics. The resonance energy and width for a broad resonance are not defined uniquely and there are many prescriptions, which have been used in the literature [35]. Not only do the definitions depend on the model used (e.g., potential, R-matrix, microscopic) but also within a given model the prescriptions for the resonance parameters can differ [35,36]. For example, in Ref. [37] four different definitions were used. In Ref. [35] two more definitions were added in the R-matrix approach. That is why we believe that, when any compilation includes the broad resonance parameters, the reference should be done to the prescriptions used to determine these parameters. The reason for this ambiguity is that for broad resonances in the physical region the nonresonant contribution becomes comparable with the resonant one. In this case the determined resonance energy and width depend on how much of the background is included into the resonant part. The only way to determine correctly the resonance energy and width is to single out the resonance pole explicitly in the function fitting the experimental data. It is realized in the S-matrix pole method.

Here we address two approaches based on the definition of the resonance energy $E_R = E_0 - i\,\Gamma/2$ as the energy at which the S matrix has a pole on the second energy sheet (low half of the momentum plane): the potential approach based on the solution of the radial Schrödinger equation and the analytical expression for the S matrix. The first one gives the most accurate definition of the resonance energy and width within the potential model, while the second one even more general because it based only on the analyticity and the symmetry of the S matrix [25].

We remind that a resonance corresponds to the pole of the S matrix at $k_R = k_0 - i\,k_I$ and is located in the fourth quadrant of the momentum complex plane. Correspondingly, the resonance energy is

$$E_R = \frac{k_R^2}{2\,\mu} = E_0 - i\,\frac{\Gamma}{2}, \tag{16}$$

where

$$E_0 = \frac{k_0^2 - k_I^2}{2\,\mu} \tag{17}$$

and

$$\Gamma = \frac{2\,k_0\,k_I}{\mu}. \tag{18}$$

For broad resonances k_I becomes comparable with k_0 or even larger ($k_0 \lesssim k_I$). If $k_I > k_0$ (i.e., the resonant pole in the complex momentum plane, due to large k_I, is far from the real energy axis) the energy of the broad resonance $E_0 < 0$ is located in the third quadrant on the second energy sheet and we call it the subthreshold broad resonance.[2] Due to large k_I (or resonance width Γ), the impact of the resonant pole on the cross section or scattering phase shift is weakened and the nonresonant amplitude or phase shift (nonresonant background) becomes important. The general expression for the elastic scattering S matrix based on its analyticity and symmetry in a vicinity of a single resonance can be written as [25]

$$\begin{aligned} S(k) &= e^{2\,i\,\delta(k)} = e^{2i\,\delta_p(k)}\,\frac{(k-k_R^*)(k+k_R)}{(k-k_R)(k+k_R^*)} \\ &= e^{2\,i\,[\delta_p(k)+\delta_R(k)+\delta_a(k)]}. \end{aligned} \tag{19}$$

where $\delta_p(k)$ is the nonresonant scattering phase shift,

$$\delta_R(k) = -\arctan\frac{k_I}{k-k_0} \tag{20}$$

$$= -\left[\frac{\pi}{2} - \arctan\frac{k-k_0}{k_I}\right], \tag{21}$$

is the resonant scattering phase shift,[3] and

$$\delta_a(k) = -\arctan\frac{k_I}{k+k_0}. \tag{22}$$

For narrow resonances, $k_I \ll k_0$, the phase shift $|\delta_a(k)| \ll 1$ can be neglected. In this case, the standard method, which we call the phase shift method (or "$\delta = \pi/2$" rule), entails the resonance energy E_0 the value at which the scattering phase $\delta(k)$ passes through $\pi/2$. The resonant width is evaluated from the formula $\Gamma = 2/(d\delta/dE)$ at $E = E_0$ or as the energy interval corresponding to change of δ from $\pi/4$ to $3\pi/4$. However, for broad resonances $\delta_a(k)$ cannot be neglected and the total nonresonant scattering phase shift $\delta_p(k) + \delta_a(k)$ becomes dependent on the resonant parameters. This nonresonant scattering phase shift may be a large negative so that the total phase shift $\delta(k)$ cannot reach $\pi/2$ at $k = k_0$, making the $\pi/2$ method nonapplicable. When calculating the elastic cross section or scattering phase shift in the presence of the broad resonance, due to the importance of the nonresonant phase shift, the cross section depends not only on the resonance parameters E_0 and Γ but also on the potential adopted.

Here as a test case we select resonances representing the ground state $1/2^+$ and the first exited state $5/2^+$ in ^{15}F. The latest very detailed analysis of the angular distributions for the ^{14}C$(d,p)^{15}$C reaction [38,39] shows that the spectroscopic factors for the ground $1/2^+$ and the first excited state $5/2^+$ are close to the single particle ones (0.99 and 0.90 correspondingly [39]). One expects the similar numbers for the mirror states in ^{15}F. Therefore, the potential approach is appropriate to describe these states. In Ref. [40] the Woods-Saxon potential parameters to describe the excitation energies of the mirror levels in ^{15}C and ^{15}F, as well as the experimental data on resonance ^{14}O + p, were found. The authors [40] presented the final data on the resonance parameters for the first two levels in ^{15}F using the calculations of the wave function inside the nucleus at the radius of 1 fm. The energy at which the

---

[2] In literature another definition of the subthreshold resonance is also being used: the resonance is subthreshold if in the resonance reaction $\alpha \to \beta$ the resonance energy in the initial channel is negative.

[3] Note that Eq. (20) is valid for any k_I for $k - k_0 \geqslant 0$ while Eq. (21) is valid for $k_I > 0$ and any $k - k_0$.

TABLE I. Energy and width of the resonances for the ^{15}F states with $J^p = 1/2^+$ (the ground state) and $5/2^+$ (the first exited state) calculated by the use of three different methods (see the text).

J^p	E_0 (MeV)	Γ (MeV)	Method
$1/2^+$	1.450	1.276	$\delta = \pi/2$
	$1.290^{+0.08}_{-0.06}$	0.7	$\lvert\Psi_{\max}\rvert$
	1.198	0.530	Pole of S matrix (potential)
	1.194	0.531	Pole of S matrix, Eq. (19)
	1.400	0.700	R matrix (from the scattering phase shift)
	1.315	0.679	R matrix (from the excitation function, $r_0 = 4.5$ fm)
	1.274	0.510	R matrix (from the excitation function, $r_0 = 6.0$ fm)
$5/2^+$	2.805	0.304	$\delta = \pi/2$
	2.795 ± 0.045	0.298 ± 0.06[a]	$\lvert\Psi_{\max}\rvert$
	2.780	0.293	Pole of S matrix
	2.777	0.286	R matrix (from the excitation function, $r_0 = 4.5$ fm)
	2.762	0.297	R matrix (from the excitation function, $r_0 = 6.0$ fm)

[a] It was misprint $\Gamma = 0.325$ MeV for the state $\frac{5}{2}^+$ in Ref. [40].

absolute value of the wave function reaches its maximum was identified as the resonance energy. We call this the $|\Psi_{\max}|$ method. In Ref. [40] the width of the resonance was defined by the energy interval over which the amplitude falls by $\sqrt{2}$ relative to the maximum of the $|\Psi_{\max}|$. For comparison, in Ref. [40] some results were presented using also the $\pi/2$ method.

We apply the potential S-matrix pole method by solving the Schrödinger equation with the Woods-Saxon potential given in Ref. [40] for both ^{15}F resonance states with the $J^\pi = 1/2^+$ and $5/2^+$. We search for the complex energy at which the coefficient $C_l^{(-)} = 0$ [see Eq. (7)] similar to the search for the bound or the virtual state. We note that in the standard approach the scattering wave function is calculated at real energies, where the nonresonant contribution is significant for broad resonances, while the Gamow wave function is calculated at the complex energy corresponding to the resonant pole of the S matrix located on the second Riemann energy sheet. As a first approximation, to determine the complex resonance energy $E_R^1 = E_0^1 - i\Gamma^1/2$, we use the phase-shift method (or the $|\Psi_{\max}|$ method when the $\delta = \pi/2$ method is nonapplicable). After that, we solve the Schrödinger equation near the complex energy $E_R^1 = E_0^1 - i\Gamma^1/2$. The final result of this search is the complex energy E_R, at which the coefficient of the incoming wave vanishes. We also applied the S-matrix pole search using the analytical representation (19) for the S matrix (see explanation below).

Our results for the energies and widths of the resonance states are given in Table I compared with the previous results obtained using the $\delta = \pi/2$ and $|\Psi_{\max}|$ methods [40]. The position E and the width Γ of the broad resonance depend on the calculation method: the S matrix pole method gives the values of the resonance energy and width smaller and more accurate than the $\delta = \pi/2$ and $|\Psi_{\max}|$ methods. It is worth noting that the corrected value of 1.227 MeV for the resonance energy of the ground state of ^{15}F is very close to the lower limit given by Fortune [32] obtained using the isobaric multiplet mass equation. Moreover, in the most recent experimental work on ^{15}F [41] it was indicated that the ground state energy of ^{15}F can be even lower.

Figures 3 and 4 show the real and imaginary parts of the normalized Gamow wave function for the $1/2^+$ and $5/2^+$ resonance states in ^{15}F. The solution of the Schrödinger equation coincides with the outgoing wave outside the potential area. We conclude that the probability of finding the proton inside the potential area is relatively high. The advantage of our method is that we directly find the complex energy of the resonant state (energy and width) by the same procedure as for the bound state.

An important test of our method is comparison of the single-particle ANC determined as an amplitude of the tail of the normalized Gamow function with the ANC determined from the residue of the scattering amplitude at the pole corresponding to the resonance. For the normalization of the Gamow wave function we use here the method suggested by Zeldovich [5], the numerical application of which is difficult for a broad resonance. However, the same relationship between the squared single-particle ANC and the residue can be used for both the bound and resonance states. One can use Eq. (15) to find the single-particle ANC of the

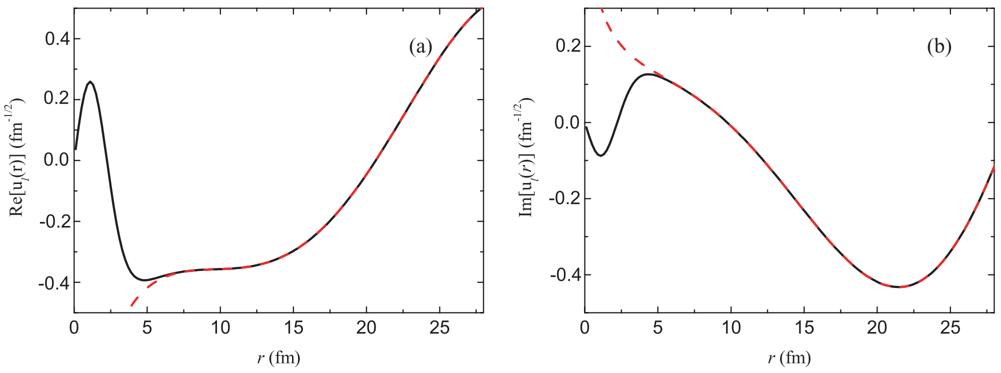

FIG. 3. (Color online) Real (a) and imaginary (b) parts of the wave function of the $1/2^+$ resonance state in ^{15}F. The solid line is the solution of the Schrödinger equation; the dashed line is the outgoing Coulomb function (the Whittaker function).

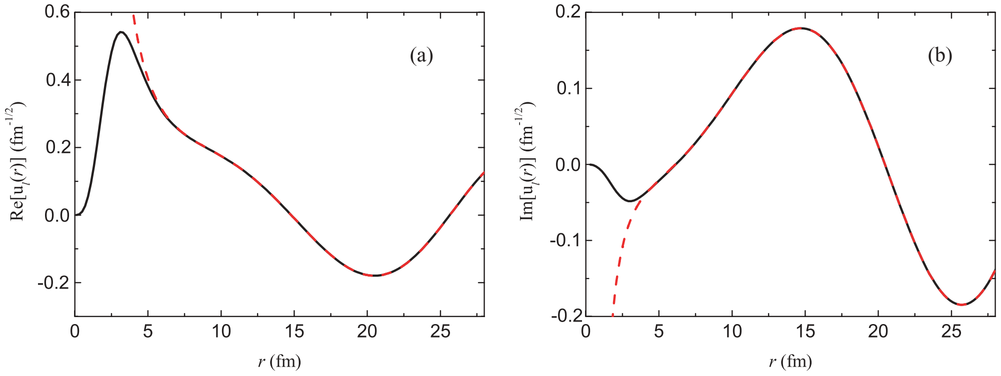

FIG. 4. (Color online) The same as in Fig. 3 but for the $5/2^+$ resonance state in ^{15}F.

resonance wave function. The results of the calculated residues are $(-0.038 + i\,0.008)$ fm^{-1} and $(0.015 - i\,0.009)$ fm^{-1} for the $1/2^+$ and $5/2^+$ states, respectively. From Eq. (15) we get the single-particle ANCs $(-0.123 + i\,0.153)$ fm$^{-1/2}$ and $(0.115 + i\,0.067)$ fm$^{-1/2}$ for the same states, correspondingly. We obtained the same single-particle ANCs directly from the tail of the normalized Gamow wave functions validating Eq. (15).

1. Model-independent determination of the energy and width of the broad resonance $\frac{1}{2}^+$ in ^{15}F

The limitations of the potential model and the existence of the phase-equivalent potentials calls for a cross-check of the energy and width for the broad resonance determined from the potential approach. We demonstrate how to determine these resonance parameters using the model-independent representation of the elastic-scattering S-matrix given by Eq. (19). Since the experimental $2s_{1/2}$ phase shift for $^{14}\mathrm{O} + p$ scattering in the resonance energy region is not available, we generate the "quasi-experimental" $2s_{1/2}$ phase shift using the Woods-Saxon potential from Ref. [40], which reproduces the $^{14}\mathrm{O} + p$ resonance scattering. Its geometry is $r_0 = 1.17$ fm, $a = 0.735$ fm, $r_C = 1.21$ fm and the depth $V_0 = 53.52$ MeV. The phase shift is shown in Fig 5. Using the S-matrix pole method from the solution of the Schrödinger equation we find the resonance energy for this potential $E_0 = 1.198$ MeV and the resonance width $\Gamma = 0.530$ MeV. Now we demonstrate that using Eq. (19) we can fit the "quasi-experimental" phase shift and determine the resonance energy and width. The potential phase shift in Eq. (19) is approximated by the polynomial $\delta_p(k) = \sum_{n=0}^{3} b_n (k - k_s)^n$. So, we have six fitting parameters including four coefficients b_n, E_0, and Γ. The final result does not depend on the choice of the center of the Taylor expansion k_s and is practically not sensitive to the starting values of E_0 and Γ. We take here the starting values $k_s = 0.25$ fm^{-1}, $E_0 = 1.45$ MeV, and $\Gamma = 1.276$ MeV obtained from the $\delta = \pi/2$ method, Table I. The fit to the "quasiexperimental" phase shift gives the final resonance energy $E_0 = 1.194$ MeV and $\Gamma = 0.531$ MeV, which is in perfect agreement with the results obtained using the potential S-matrix pole method. For the starting search values $E_0 = 1.6$ MeV and $\Gamma = 1.276$ MeV we get the fitted energy $E_0 = 1.198$ MeV and $\Gamma = 0.532$ MeV. Thus Eq. (19) allows one to obtain the energy and width of the broad resonance using, for example, as input parameters the resonance and width obtained by the $\delta = \pi/2$, $|\Psi_{\max}|$. The model-independent result obtained from Eq. (19) gives very close values to the potential S-matrix pole. Assigning a 10% uncertainty to the "quasiexperimental" phase shift results in a similar uncertainty in the determined "quasiexperimental" phase-shift resonance energy and width.

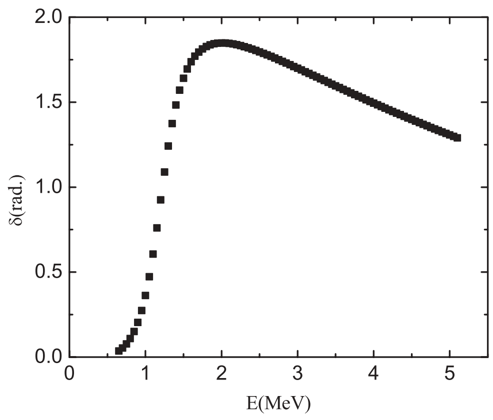

FIG. 5. The $^{14}\mathrm{O} + p$ $2\,s_{1/2}$ scattering phase shift generated by the Woods-Saxon potential from [40] and used as the "quasiexperimental phase shift."

2. Comparison with R-matrix approach

The resonant S matrix obtained from the R matrix contains the nonresonant contribution through the energy dependence of the level shift and resonance width. The extrapolation of this functions to the complex energy plane make them complex, i.e., they lose it physical meaning. Thus the R-matrix approach is not designed for extrapolation to the resonant pole.

Here we apply the R-matrix approach to determine the energy and the width of the resonance with the S-matrix pole method. For an isolated resonance in the single-level, single-channel R-matrix approach with the zero boundary condition the Coulomb-modified nuclear scattering S matrix is

$$S = e^{2\,i\,\delta_{hs}}\,\frac{E_0 - E + i\,\frac{\Gamma(E)}{2}}{E_0 - E - i\,\frac{\Gamma(E)}{2}}, \tag{23}$$

where δ_{hs} is the hard-sphere scattering phase shift. To obtain this equation the linear energy dependence of the level shift function $\Delta(E)$ is taken into account [42]. Here, E_0 is the real part of the resonance energy. In the R matrix E_0 is determined as $E_\lambda + \Delta(E_0) = E_0$, E_λ is the R-matrix level energy, and $\Gamma(E) = 2\,\gamma_l^2\,P_l^2(E, r_0)$ is the observable resonance width in the R-matrix approach depending on the energy and the channel radius r_0, γ_l is the observable reduced width amplitude, $P_l(E, r_0)$ is the penetrability factor in the l-th partial wave. The resonance width in the R-matrix approach, in contrast to the Breit-Wigner equation, depends on the energy. This dependence reflects the fact that the S matrix in the R matrix is richer than the Breit-Wigner equation: it includes also the nonresonant background, which is contributed by the hard-sphere phase shift and the energy dependence of the level shift function and the resonance width. For narrow resonance $[\Gamma(E_0) \ll E_0)]$ the pole in Eq. (23) $E_R \approx E_0 - i\,\Gamma(E_0)/2$. For a broad resonance this resonance energy is not a pole of the S matrix. The equation for the resonant pole in this case is given by $E_R = E_0 - i\,\Gamma(E_R)/2$. At complex E_R $\Gamma(E_R)$ becomes complex and loses its meaning of the width. For a broad resonance in the R-matrix method the resonance energy is defined as $E_R = E_0 - i\,\Gamma(E_0)$, which is not a pole of Eq. (23). Hence, for broad resonances the difference between the resonance energy from the S-matrix pole method and the R-matrix method is expected.

To compare the results for the R-matrix and S-matrix pole methods for the ${s_{1/2}}^+$ resonance we use the phase shift generated by the Woods-Saxon potential from Ref. [40] as the "quasiexperimental" one and determine the resonance energy and width by fitting the R-matrix phase shift to the "quasi-experimental." The results are shown in Table I. The R-matrix resonance energy and width found at $r_0 = 5.0$ fm are higher than the S-matrix pole ones and close to the $|\Psi_{\rm max}|$ result. Both R-matrix and $|\Psi_{\rm max}|$ methods determine the resonance energy from the data at real energies where for broad resonances the contribution of the background becomes important. The S-matrix pole method determines the resonance energy and width by extrapolating the data to the pole in the complex energy (momentum) plane. In the vicinity of the pole the resonant contribution becomes dominant compared to the background and determination of the resonance parameters is more accurate than in the physical region.

We made additional comparison of the R-matrix approach by fitting the measured in [40] the excitation function of the $^{14}\mathrm{O} + p$ scattering at 180°. Both resonances ${s_{1/2}}^+$ and ${d_{5/2}}^+$ coherently contribute to the excitation function. The resonances can be separated only after integration over the scattering angle. The selection of 180° scattering angles minimizes the Coulomb scattering effects and enhances the $d_{5/2}^+$ resonance contribution. The two-level R-matrix fitting to the excitation function gives the observable resonance energy and width presented in Table I for two channel radii $r_0 = 4.5$ and 6 fm. The resonance energy is determined as the peak of the $|S(k) - 1|^2$, and the width as the full width at half maximum of this function. We note that this prescription differs from two prescriptions used in Ref. [36]. For narrow ${d_{5/2}}^+$ all methods gives very close results, but it is not the case for the broad resonance ${s_{1/2}}^+$. The R-matrix results are between the $|\Psi_{\rm max}|$ and the S-matrix pole. Since the S-matrix pole method based on Eq. (19) correctly takes into account the resonance contribution as a pole in the complex energy (momentum) plane and analytically continue it to the physical region, it allows one to separate correctly the nonresonant (background) contribution from the resonance one and, hence, provides the most accurate determination of the resonance energy and width.

D. The lowest levels in the mirror nuclei ^{11}Be and ^{11}N

The light neutron-rich nucleus ^{11}Be is probably the most discussed nucleus. The interest to ^{11}Be is related to the well-known inversion of the shell-model levels in this nucleus. It has the following low-lying states: $\frac{1}{2}^+$ (ground state) and the excited states $\frac{1}{2}^-$ at $E_x = 0.320$ MeV and $\frac{5}{2}^+$ at $E_x = 1.778$ MeV [43]. The first two are the bound states while the third one is a resonance. As it was mentioned in Ref. [13] "the lowering of the $s_{1/2}$ orbital with respect to the $0d_{5/2}$ orbital is expected for a simple potential well." The $p_{1/2}$ state belonging to the $K = 1/2$ band has a pretty stable dominantly [421] spatial symmetry configuration since the next $1/2^-$ state is 10 MeV away [44]. In Ref. [45] was shown that that the lowest $p_{1/2}$ state obtained in a central potential with the spin-orbital interaction strongly overlaps with the state projected from a Slater determinant of the lowest orbits in the Nilsson's model with the same spin-orbital interaction as in the shell model and deformation.

In this work to test our method we apply it for calculation of the three lowest states $s_{1/2}$, $p_{1/2}$, and $d_{5/2}$ in ^{11}Be and ^{11}N nuclei belonging to the multiplet $T = 3/2$. We also estimate the spectroscopic factors for $s_{1/2}$ and $d_{5/2}$ states using the potential approach leaving aside $p_{1/2}$ state, which is not a single particle [13].

Different reactions, including the $^{10}\mathrm{Be}(d,p)^{11}\mathrm{Be}$ reaction with the radioactive ^{10}Be target, were used to obtain the spectroscopic factors for the lowest states in ^{11}Be. As a standard procedure, the single-particle neutron wave functions in ^{11}Be are used as the input in the DWBA code to get the neutron spectroscopic factors. The obtained spectroscopic factors are in the intervals (0.5–0.96) [46] and (0.7–0.8) [47]. But they are model dependent because they depend on the Woods-Saxon potential adopted for the neutron bound state in ^{11}Be, optical potential in the initial and final channels of the (d,p) reaction, and accuracy of the DWBA to analyze for the deformed ^{11}Be [48]. *A priori* the transfer reactions involving deformed nuclei require the codes, which take into account the multistep transfer mechanisms, for example, the coupled-channels Born approximation available in FRESCO. That is why it is difficult to say from the DWBA analysis to what extent the three lowest neutron states are single particle.

The nucleus ^{11}N is the mirror of ^{11}Be, and it should have a similar level scheme. All states ^{11}N are unstable to proton decay. Therefore, their decay widths directly related to their single-particle nature. Since the discovery of the ground state in ^{11}N in 1996 [49], the lowest levels in ^{11}N were studied in many works (see Ref. [50] and references therein). In this section, we apply the S-matrix pole method to study the broad

TABLE II. Energies and widths calculated for low-lying levels of ^{11}Be by S-matrix pole method ($r_{ls} = r_0$, $a_{ls} = a$).

J^π	r_0 (fm)	a (fm)	V_0 (MeV)	V_{ls} (MeV)	$E_{\rm sp}$ (MeV)	$\Gamma_{\rm sp}$ (MeV)
$\frac{1}{2}^+$	1.20	0.753	57.057	0	−0.503	Bound
	1.22	0.713	57.057	0	−0.503	Bound
	1.25	0.650	57.057	0	−0.503	Bound
	1.27	0.607	57.057	0	−0.503	Bound
	1.29	0.562	57.057	0	−0.503	Bound
$\frac{1}{2}^-$	1.20	0.819	37.505	6.0	−0.183	Bound
	1.22	0.760	37.505	6.0	−0.183	Bound
	1.25	0.650	37.505	6.0	−0.183	Bound
	1.27	0.545	37.505	6.0	−0.183	Bound
	1.28	0.451	37.505	6.0	−0.183	Bound
$\frac{5}{2}^+$	1.20	0.753	57.057	7.131	1.275	0.221
	1.22	0.713	57.057	6.222	1.275	0.208
	1.25	0.650	57.057	4.743	1.275	0.189
	1.27	0.607	57.057	3.671	1.275	0.176
	1.29	0.562	57.057	2.520	1.275	0.164

TABLE III. Energies and widths calculated for low-lying levels of ^{11}N by the S-matrix pole method. The Coulomb radius $r_C = 1.1$ fm ($r_{ls} = r_0$, $a_{ls} = a$).

J^π	r_0 (fm)	a (fm)	V_0 (MeV)	V_{ls} (MeV)	$E_{\rm sp}$ (MeV)	$\Gamma_{\rm sp}$ (MeV)
$\frac{1}{2}^+$	1.20	0.753	57.057	0	1.014	0.843
	1.22	0.713	57.057	0	1.039	0.881
	1.25	0.650	57.057	0	1.081	0.944
	1.27	0.607	57.057	0	1.112	0.993
	1.29	0.562	57.057	0	1.146	1.048
$\frac{1}{2}^-$	1.20	0.819	37.505	6.0	1.919	0.944
	1.22	0.760	37.505	6.0	1.991	0.963
	1.25	0.650	37.505	6.0	2.134	0.996
	1.27	0.545	37.505	6.0	2.284	1.024
	1.28	0.451	37.505	6.0	2.426	1.047
$\frac{5}{2}^+$	1.20	0.753	57.057	7.131	3.672	0.959
	1.22	0.713	57.057	6.222	3.719	0.927
	1.25	0.650	57.057	4.743	3.793	0.878
	1.27	0.607	57.057	3.671	3.845	0.847
	1.29	0.562	57.057	2.520	3.900	0.8167

levels in ^{11}N. Simultaneously we attempt to find restrictions on the single-particle potentials related to the widths and excitation energies of the mirror states in ^{11}Be and ^{11}N.

To determine the single-particles levels in ^{11}Be and ^{11}N, we use the Woods-Saxon plus Coulomb potential similar to the ones used in Refs. [35,46,51,52]. The parameters of the potential are fitted to reproduce the energies of the low-lying levels in ^{11}Be. Then we use this nuclear potential plus the Coulomb potential to find the mirror levels in ^{11}N. We apply the pure single-particle approach as in Refs. [35,51].

The different sets of the potential parameters, which were used to fit the lowest levels in ^{11}Be, are presented in Table II. As a starting point, the standard geometrical parameters $r_0 = 1.25$ fm, $a = 0.65$ fm of the Woods-Saxon potential are used. Then, we vary the depth of the central potential V_0 to fit the binding energy of the ground state $s_{1/2}$ of ^{11}Be (well-depth procedure). After that, we vary the radius r_0 and the diffuseness parameter a to fit the binding energy in ^{11}Be at the fixed depth $V_0 = 57.057$ MeV found from the fitting at standard geometrical parameters. We use the same procedure for the $p_{1/2}$ and $d_{5/2}$ states. As is seen in Table II, the adopted potential well is shallower for the $p_{1/2}$ state than for the ground state, which reflects the inversion of the s and p levels. To reproduce the well-known energy of $\frac{5}{2}^+$ resonance ($E_R = 1.275$ MeV), we use the set of the potential parameters determined for the ground state $\frac{1}{2}^+$ of ^{11}Be with addition of the spin-orbital potential. The fact that $\frac{5}{2}^+$ state has particle width provides for an additional criterion for the selection of the potential. As can be seen in Table II, the calculated single-particle widths for this state are larger than the experimental values of 100 ± 20 keV [43] and 104 ± 21 keV [53]. Taking into account that

$$\Gamma_{\rm exp} = S\,\Gamma_{\rm sp}, \tag{24}$$

we can estimate the spectroscopic factor S for this state. Here $E_{\rm sp}$ and $\Gamma_{\rm sp}$ stand for E_0 and Γ, correspondingly. The experimental and theoretical spectroscopic factors are in the range 0.45–0.8 [47]. The spectroscopic values in the interval 0.45–0.61 are obtained by comparing the data in Table II and the experimental ones. Taking into account the experimental uncertainties of 20%, the highest value of the spectroscopic factor can be ∼0.73. (To decrease the calculated single-particle width one has to use a sharper potential [smaller diffuseness], which seems in contradiction with current experimental data and the theoretical predictions [see Ref. [40] and references therein]). Smaller experimental uncertainties in the width of the $\frac{5}{2}^+$ state result in stronger restrictions in the potential parameters.

The S-matrix pole calculations for the three states, which are all resonances, for the mirror ^{11}N nucleus are made using the potential parameters for the ^{11}Be nucleus by adding the Coulomb potential of the uniformly charged sphere of the radius parameter r_C [Eq. (2)]. The results are shown in Tables III and IV for two values of the radius of the uniformly charged sphere.

It is worth noting that in the case of the relatively sharp $\frac{5}{2}^+$ resonance, the differences between calculations of the resonance energy and the width using the S-matrix pole and the phase shift are relatively moderate, ∼140 keV and ∼130 keV, correspondingly. However, these differences become significantly larger for the broad resonance $\frac{1}{2}^-$ in ^{11}N, up to ∼300 keV for the energy and ∼500 keV for the width. We note that for the same set of the potential parameters the S-matrix pole method gives energy and width smaller than those obtained by the phase shift. As for the $2s_{1/2}$ state in ^{11}N, the phase shift never passes through $\pi/2$ in agreement with the earlier observation by Barker [35].

The S-matrix pole method reveals the resonance pole for the state $\frac{1}{2}^+$ in ^{11}N. To check that we have found the pole correctly and match the logarithmic derivatives of the solution of the Schrödinger equation and the Gamow function

TABLE IV. The same as in Table III but for the Coulomb radius $r_C = 1.2$ fm ($r_{ls} = r_0$, $a_{ls} = a$).

J^π	r_0 (fm)	a (fm)	V_0 (MeV)	V_{ls} (MeV)	$E_{\rm sp}$ (MeV)	$\Gamma_{\rm sp}$ (MeV)
$\frac{1}{2}^+$	1.20	0.753	57.057	0	0.999	0.803
	1.22	0.713	57.057	0	1.022	0.837
	1.25	0.650	57.057	0	1.062	0.896
	1.27	0.607	57.057	0	1.096	0.942
	1.29	0.562	57.057	0	1.129	0.993
$\frac{1}{2}^-$	1.20	0.819	37.505	6.0	1.902	0.920
	1.22	0.760	37.505	6.0	1.972	0.936
	1.25	0.650	37.505	6.0	2.110	0.963
	1.27	0.545	37.505	6.0	2.252	0.986
	1.28	0.451	37.505	6.0	2.386	1.002
$\frac{5}{2}^+$	1.20	0.753	57.057	7.131	3.655	0.945
	1.22	0.713	57.057	6.222	3.701	0.912
	1.25	0.650	57.057	4.743	3.773	0.864
	1.27	0.607	57.057	3.671	3.823	0.832
	1.29	0.562	57.057	2.520	3.875	0.801

in the asymptotic region. We also check the ratio of the solution to the Gamow function, which must be constant at the asymptotic region. Let us consider the $\frac{5}{2}^+$ level in ^{11}N. By averaging the experimental data from Refs. [49,54–56], we obtain 3.72 ± 0.050 MeV for the resonance energy for this level and $0.55^{+0.05}_{-0.1}$ MeV for the width. We can conclude from Tables III and IV that the S-matrix pole method gives for the width ~0.878 MeV resulting in the spectroscopic factor $S = 0.63$. The standard geometrical parameters $r_0 = 1.25$ fm and $a = 0.65$ fm provide for a good agreement with the average experimental energy for this level. Using these parameters (Table II), one can find the spectroscopic factor of 0.53 for the mirror state in ^{11}Be. Assuming that the spectroscopic factors should be the same for the mirror states, one can conclude that the average value of the spectroscopic factor $S = 0.58$ is a characteristics of the single-particle structure for the $\frac{5}{2}^+$ state in the mirror ^{11}N and ^{11}Be nuclei.

The experimental data for the broad $\frac{1}{2}^-$ resonance state in ^{11}N need careful consideration because the results reported in Refs. [49,50,55,56] are different due to different definitions of "energy" and "width" in these works. We nevertheless conclude that the resonance energy of this state is ~2.15 MeV. As in Ref. [44] we use Eq. (24) to get the width of the $\frac{1}{2}^-$ state in the potential approach. The spectroscopic factor $S = 0.66$ results in the width $\Gamma = 0.65$ MeV for this state. This spectroscopic factor coincides with the shell-model prediction for the analog state of ^{11}Be and our result is in a good agreement with the one obtained in Ref. [44].

All available experimental data [49,50,56] give higher resonance energies of the $\frac{1}{2}^+$ state in ^{11}N than our calculations (see Table III and IV). (We exclude most of the mass-transfer data from the consideration because of the very low population of the $\frac{1}{2}^+$ state in ^{11}N in these reactions.) The ^{11}N ground state resonance energies (the relative ^{10}C + p energy) are grouped around 1.3 MeV from the data [50,56]. The most recent study [56] resulted in the value of 1.54 MeV for the resonance energy; the experimental widths for the resonance are in the range from 0.83 MeV [56] to 1.4 MeV [50]. These experimental values were extracted using different approaches. In Refs. [49,50] the behavior of the single-particle wave function inside the ^{11}N nucleus is used to determine the resonance energy (identified as the energy at which the modulus of the wave function calculated at 1 fm reaches maximum, the $|\Psi_{\rm max}|$ method) and the resonance width. The R-matrix analysis was used in Ref. [56]. Both approaches cannot eliminate a contribution from the nonresonant potential scattering. Leaving a detailed analysis of the experimental data for future studies, we make a crude estimation of the spectroscopic factor for the 2s state. To this end we average data from Refs. [49,50] for the $\frac{1}{2}^+$ resonance getting the resonance energy 1.30 MeV and resonance width 1.20 MeV. The analysis [49,50] was based on a potential approach, i.e., the Woods-Saxon potential was found, which allows fitting the excitation functions and angular distributions for the elastic proton resonance scattering. Using the potential parameters from Ref. [49], we apply here the S-matrix pole method, rather than the $|\Psi_{\rm max}|$ method, to determine the resonance energy and width. We obtain 1.102 MeV for the resonance energy and 840 keV for the resonance width, i.e., the resonance energy of $\frac{1}{2}^+$ state in ^{11}N decreases by 200 keV compared to the one adopted previously. We now adopt 1.102 MeV as a new "experimental" resonance energy of the $\frac{1}{2}^+$ state in ^{11}N.

We note that the potential found in Ref. [49] does not reproduce the experimental binding energy of the $\frac{1}{2}^+$ state and resonance energy of $\frac{5}{2}^+$ state in ^{11}Be. Meanwhile the potentials given in Tables III and IV fit 2s and 1d states both in ^{11}Be and ^{11}N. Then, we assume that the potential with the standard geometry $r_0 = 1.25$ fm and $a = 0.65$ fm in Table IV is the "right" one. Note that the resonance energy and width obtained for this potential are very close to the average resonance energy and width shown in Table IV for five different potentials. This potential gives 1.062 MeV resonance energy, which is a pure single-particle energy. We observe that this energy is ~0.04 MeV less than the "experimental" value of 1.102 MeV obtained for the potential adopted in Ref. [49]. This 0.04 MeV can be attributed to the non-single-particle admixture to the structure of the $\frac{1}{2}^+$ state ^{11}N.

An estimation of the spectroscopic factor can be obtained from the consideration of the width of the state. The $r_0 = 1.25$ fm and $a = 0.65$ fm parameters generate 0.92 MeV for the $\frac{1}{2}^+$ state width at the "experimental" resonance energy of 1.102 MeV. The ratio of 0.92/0.896 (the "experimental" width/calculated width) results in the spectroscopic factor of 1.03 for the adopted potential with the standard geometry. Hence we obtain much larger spectroscopic factors for the ground state in ^{11}N than for the $\frac{5}{2}^+$ excited state.

As a final remark to this section, it is worth noting that the conventional potential approaches, which determine the resonance energy and width from the energy dependence of the phase shift or from the $|\Psi_{\rm max}|$ method, may not give accurate results because of the distortion generated by the nonresonant background at physical energies. For example, $|\Psi_{\rm max}|$ may reach a peak in the internal region at energy $E \neq E_0$. In this sense the S-matrix pole is the most accurate method for a given potential because it determines the resonance energy and width by searching the resonant pole at complex energy, i.e., separates the resonant contribution from the background. We note that the resonance energy determined by the S-matrix pole method depends on the adopted potential. Moreover, the resonance parameters determined by the S-matrix pole method may differ from the ones determined from the R-matrix approach as we have seen it for the ^{15}F case.

1. Model-independent determination of the energy and width of the broad resonance $\frac{1}{2}^+$ in ^{11}N

Here we determine the resonance parameters for the $2s_{1/2}$ resonance in $^{11}\mathrm{N} = {}^{10}\mathrm{C} + p$ using the model-independent representation of the elastic-scattering S matrix given by Eq. (19). We use the Woods-Saxon potential with the standard geometry $r_0 = 1.25$ fm, $a = 0.65$ fm, the Coulomb radial parameter $r_C = 1.2$ fm and the depth $V_0 = 57.057$ MeV to generate the “quasiexperimental” $2s_{1/2}$ phase shift. The resonance energy for this potential obtained from the Schrödinger equation is $E_0 = 1.062$ MeV and the resonance width $\Gamma = 0.896$ MeV (see Table IV). To fit this “quasiexperimental” phase shift we use the polynomial approximation $\delta_p(k) = \sum_{n=0}^{3} b_n(k - k_s)^n$ in Eq. (19). The S-matrix pole method based on Eq. (19) gives $E_0 = 1.072$ MeV and $\Gamma = 0.916$ which agrees with the potential S-matrix pole. As starting search value in fitting the “quasiexperimental” phase we used $k_s = 0.21$ fm^{-1} but the result only depends slightly on the initial k_s value.

E. ^{26}Mg-n broad resonances

Neutron resonances play an important role in nuclear astrophysics. Some of these resonances, due to the absence of the Coulomb barrier, may be quite broad. That is why it would be of interest to test the S-matrix pole methods for broad neutron resonances. Here we compare the resonant parameters for the ^{26}Mg-n system obtained in Ref. [57] using the potential approach with the S-matrix pole method and R-matrix approach. In Ref. [57] the folding potential was used to generate the potential phase shifts for the $^{26}\mathrm{Mg} + n$ p-wave scattering at different potential strength. We selected two potentials from Ref. [57] corresponding to the potential strength parameter $\lambda = 0.9$ and 1.04. The resonance energy and width obtained in Ref. [57] for these potentials are given in Table V. For both cases the resonances are quite broad, especially for smaller λ. We fitted the potential phase shifts from Ref. [57] using the analytical expression (19) (the S-matrix pole method) and the R-matrix approach at different channel radii. As in the previous sections the potential phase shift in Eq. (19) is approximated by the polynomial $\delta_p(k) = \sum_{n=0}^{3} b_n(k - k_s)^n$. The final result practically does not depend on the choice of the center of the Taylor expansion k_s. When fitting the potential phase shifts from Ref. [57] as the starting value we take $k_s = 0.3$ fm^{-1} for both λ, and for the starting values for the resonance energy and width we use the values obtained in Ref. [57]; see Table VI. As we can see both resonances are broad but the resonance at $\lambda = 0.9$ is extremely broad. It is a very instructive case because the fitting of the potential phase shift from Ref. [57] using the S-matrix pole method and R-matrix approach reproduces quite well the fitted phase shift but provides different results because of the various definitions of the resonance energy and width in different approaches. The energy of both resonances obtained in Ref. [57] and in the S-matrix pole are close but the width obtained from the S-matrix pole method almost twice smaller for $\lambda = 0.9$ than the value obtained in Ref. [57]. For $\lambda = 1.04$ the resonance is narrower and the S-matrix pole method gives energy and width close to the ones reported in Ref. [57]. Different results generate the R-matrix method. The R-matrix results are very sensitive to the variation of the channel radii. The best fit of the potential phase shifts is achieved at $r_0 = 5.9$ fm. For $\lambda = 0.9$ the R-matrix fit gives the width close to the value obtained in Ref. [57] but the resonance energies differ substantially. For $\lambda = 1.04$ the energy and width generated by the R-matrix method are larger than the S-matrix pole method results. We note that the S-matrix pole method gives always lower width than other approaches.

TABLE V. Calculated energies E_0 and widths Γ of a p-wave potential resonance for the folding potential given in Ref. [57] at two values of the strength parameter λ and results of fitting by S-matrix pole method.

λ	From Ref. [57]		S-matrix pole method	
	E_0 (MeV)	Γ (MeV)	E_0 (MeV)	Γ (MeV)
0.9	0.795	4.130	0.740	2.540
1.04	0.274	0.300	0.280	0.276

F. The subthreshold resonances in the proton-proton system

The poles for the antibound state of the singlet neutron-neutron or the neutron−proton systems are located on the imaginary axis in the complex momentum plane (at energies $E_{nn} \cong -134$ keV and $E_{np} \cong -66$ keV). In Ref. [24] using the effective-range approach Kok showed that in the case of the proton-proton system the pole moves to the complex plane, due to the Coulomb barrier. The ground state pole of the s-wave pp-scattering amplitude was found

TABLE VI. Results of fitting by R matrix the p-wave potential phase shift curves given in Ref. [57].

r_0 (fm)	$\lambda = 0.9$		$\lambda = 1.04$	
	E_0 (MeV)	Γ (MeV)	E_0 (MeV)	Γ (MeV)
5.0	2.992	7.340	0.396	0.660
5.5	2.556	5.529	0.388	0.566
5.9	2.287	4.533	0.383	0.496
6.0	2.228	4.326	0.381	0.479
6.5	1.930	3.000	0.375	0.400
7.0	1.776	2.999	0.369	0.330

in Ref. [24] at $k_{pp} = (0.0647 - i0.0870)$ fm^{-1} or $E_{pp} = (-140 - i467)$ keV. The effective-range parameters for the standard expansion were taken from Ref. [58]. Recently, calculations with the same approximation were repeated in Ref. [59] resulting in $k_{pp} = (0.0644 - i0.0871)$ fm^{-1} or $E_{pp} = (-142 - i465)$ keV, which is in a good agreement with the Kok's result.

A definition of the renormalized partial amplitude in the presence of the Coulomb interaction was given earlier (see Eq. (3) in Ref. [60]). A new corresponding formula was derived in Ref. [59] for the renormalized vertex constant G_{ren} for the virtual decay of a nucleus into two charged particles in the effective-range theory. It was applied to the *pp* and *pd* systems using the standard effective-range expansion and the effective-range function with a pole, respectively. The value of G^2_{ren} is real quantity for the bound state because the energy is real. In the case of the resonance, the energy is complex so G^2_{ren} becomes complex. For the *pp* ground state, the value $G^2_{\text{ren}} = (0.060 + i0.051)$ fm was obtained in Ref. [59] with the effective-range parameters taken from Ref. [58]. The only condition which validates these results is the convergence of the effective-range expansion near the pole considered. It was shown in Ref. [24] that the results change only slightly when the parameters of form are neglected ($P = Q = 0$). The convergence is ensured in the case of the *pp* subthreshold resonance pole.

Nevertheless, the effective-range approximation has some drawbacks. It gives the partial scattering amplitude in an analytical form as a ratio of two polynomials. As a result, all the amplitude singularities are poles in the complex momentum plane. The number n of the poles is obviously defined by the maximal degree used in the effective range expansion up to k^n, which gives the degree of Kok's equation for the position of the pole and, correspondingly, the number of its solutions without the Coulomb force. For example, a logarithmic dynamical cut of the amplitude in the case of the two-body model with the Yukawa potential cannot be reproduced in this approximation. But it is imitated by a pole located on the positive imaginary axis, which is not a bound-state pole. In the case of the *pp* system, the situation is simple because there is no bound state, so any pole on the positive energy axis is an unphysical one. Moreover, the region of the validity of the effective-range approximation is limited by the condition $|k| \leqslant |k_{\max}|$, where the effective-range expansion converges. In the potential model with the asymptotic $V(r) \to \text{const.} \times r^{\nu} \times \exp(-r/R)$, the value $|k_{\max}| = 1/(2R)$ is the beginning of the dynamical cut on the imaginary axes in the complex k plane. In the case of charged particles, the number of roots is infinite (see Ref. [61]). In particular, as noted in Ref. [61], the sequence of poles located near the negative imaginary axis can be mistakenly identified as virtual (antibound) state poles known for the system without the Coulomb interaction.

Finding the pole by solving the Schrödinger equation is the most reliable way to confirm that the pole found by a solution of Kok's equation [24] is not a false one. This was done in the present article for the *pp* system with the Yukawa potential. Its parameters are taken from Ref. [58] for the singlet *np* system. We find that $k^{Yu}_{pp} = (0.064 - i\,0.082)$ fm^{-1} [or $E_{pp} = (-106.7 - i\,435.5)$ keV] for the *pp* ground state. After that, we have slightly changed the geometric parameter to describe the experimental *pp*-scattering length and effective range and the resolved Schrödinger equation gives $E_{pp} = (-138.16 - i\,463.14)$ keV. This result almost coincides with Kok's results. The pole for *nn* system is $E_{nn} = -92$ keV. The resonance wave function contains the outgoing wave in the asymptotic region while the ingoing wave is absent. For the normalization of the wave function in this case we cannot use the Zeldovich procedure because $\text{Re}(k_{pp}) < \text{Im}(k_{pp})$, however, we can find residue at the pole. The residue in the pole corresponding to the subthreshold resonance is $A_{pp} = (-0.021 + i0.057)$ fm^{-1}.

IV. ACCURACY OF CALCULATIONS

In the standard programs included in MATHEMATICA package numerical calculations can be performed with the very high precision of about 10^{-16} and even higher. Before using this package, we compared the results of the numerical solutions of the Schrödinger equation with the analytical results known for the Hulthén potential. In this two-body model, the relative accuracy of our binding energy calculations is 10^{-7} for the ground state and 10^{-4} for the virtual state of ^{3}H. For the virtual state, the accuracy is less due to the exponential increase of its wave function in the asymptotic region. In the second step we construct the incoming and outgoing Coulomb waves using of the hypergeometric functions $U(a, b; x)$ of the MATHEMATICA package and define the regular $F_l(\eta, x)$ and irregular $G_l(\eta, x)$ Coulomb functions. We insert these functions into the Schrödinger equation with the Coulomb potential and obtain results with an accuracy of about 10^{-10} for $u_l^{(+)}$ and G_l functions at $x = 1$ and $\eta = 6 + 2i$. For other functions, there is even greater accuracy. We also compare our calculated values of F_0 and G_0 with the values given in the tables in Ref. [62]. All digits coincide with the table data. One of the ways to check is to use the Wronskian. The calculated Wronskian coincides with the exact value with an accuracy of 10^{-16}.

We use the condition $C_l^{(-)} = 0$, Eq. (7), to find the pole of the Schrödinger equation. This means that the solution matches the outgoing wave at a distance larger than the radius of the nuclear potential. The program stops searching zero if $|C_l^{(-)}/C_l^{(+)}| < 10^{-5} - 10^{-4}$. We compare the logarithmic derivative of the solution and the outgoing wave at $R_{\max}$ as well. As a rule, these derivatives coincide with accuracy higher than 10^{-4}. Finally, we check the ratio of the solution and the outgoing wave, starting from the radius of the nuclear potential up to $2 - 3\ R_{\max}$ (see Figs. 1–4). This ratio is constant with an accuracy better than 10^{-3}.

In conclusion, we note our method provides accuracy much higher than 10^{-4}, but for nuclear physics the achieved accuracy is more than appropriate.

V. CONCLUSION

In the present work we apply the *S*-matrix pole method to determine the energies of the bound, the virtual states, and resonances. This method is based on a numerical solution of the Schrödinger equation. Usually this method is applied to the bound states, but here it is extended to the resonance and virtual states despite the fact that the corresponding solutions increase exponentially when $r \to \infty$. The method turns out to be especially useful for broad resonances including subthreshold ones.

There can be a few poles in the complex plane when applying the effective range theory and the number of the poles is defined by the maximal power k^n used in the effective range expansion. An additional investigation should be done to select a physical pole. In our approach one gets no false poles, thus resolving ambiguity problem appearing in the effective range approach.

In the case of the resonances potential models and R-matrix approach are commonly used to analyze the experimental data, and resonance parameters are determined from the fits. For narrow resonances both approaches give accurate results. However, this is not the case for broad resonances. In this case, due to the distortion caused by the nonresonant background at physical energies, the resonance energy and the width determined from the fitting of the experimental data depend on the model and within a given model the prescriptions to determine the resonance energy and width may be different. Usually researchers use different definitions of the resonance energy and width. Broad resonance parameters extracted from the experimental data are model dependent. For this reason, one should indicate the method used to determine them in any subsequent references.

Here we address two methods for determining the resonance energy and width from the pole of the S matrix: the potential S-matrix pole method based on the solution of the Schrödinger equation and the S-matrix pole method based on the analytical continuation for the S matrix to the resonant pole. We compare the results for the resonance parameters obtained from the different determinations of the resonance energy and width in the potential approach, the S-matrix pole methods and R-matrix method. Correct evaluations of the resonance parameters are important when comparing the experimental data, both for the tests of the isobaric multiplet mass equation and for detailed structure calculations of the exotic nuclei. The potential S-matrix pole method provides the most accurate resonance energy and width for a given potential. The second S-matrix pole method, which uses Eq. (19), is even more general because it does not require any potential model and is based only on the analyticity and symmetry of the S matrix. In contrast to other approaches, the pole S-matrix methods allow one to correctly separate the resonance pole contribution and the nonresonant background.

Our approach has a potential of being extended to treat broad resonance populated in transfer reactions, where the half-off-energy shell-resonant amplitude interferes with the half-off-energy shell-nonresonant amplitude. At present there is a huge disagreement in the resonance parameters for broad resonances obtained from the resonance or direct reactions [50].

APPENDIX

As the input data for calculations, we use the nuclear masses from Ref. [63]: neutron mass $m_n = 939.565$ MeV; proton mass $m_p = 938.272$ MeV; beryllium ^{10}Be mass $m_{^{10}\mathrm{Be}} = 9325.577$ MeV; carbon ^{13}C mass $m_{^{13}\mathrm{C}} = 12109.577$ MeV; carbon ^{10}C mass $m_{^{10}\mathrm{C}} = 9327.646$ MeV; oxygen ^{14}O mass $m_{^{14}\mathrm{O}} = 13044.94$ MeV. Pion mass is taken to be $m_\pi = 135$ MeV. In subsection F we use $m_N = 938.686$ MeV to be in agreement with the value $\hbar^2/m_N = 41.47$ MeV fm^2 [24].

ACKNOWLEDGMENTS

The work was supported by the US Department of Energy under Grant No. DE-FG02-93ER40773 and DE-FG52-06NA26207, NSF under Grant No. PHY-0852653, the Russian Foundation for Basic Research, Project No. 07-02-00609, and the HEC of Pakistan under Grant No. 20-1171-R.

[1] K. Möller and Yu. V. Orlov, Fiz. Elem. Chastits At. Yadra **20**, 1341 (1989) [Sov. J. Part. Nucl. **20**, 569 (1989)].

[2] Yu. V. Orlov and V. V. Turovtsev, Zh. Eksp. Teor. Fiz. **86**, 1600 (1984) [Sov. Phys. JETP **86**, 934 (1984)].

[3] J. Aguilar and J. M. Combes, Commun. Math. Phys. **22**, 269 (1971); E. Baslev and J. M. Combes, *ibid.* **22**, 280 (1971); B. Simon, *ibid.* **27**, 1 (1972); Ann. Math. **97**, 247 (1973).

[4] B. Gyarmati and A. T. Kruppa, Phys. Rev. C **34**, 95 (1986).

[5] Ya. B. Zeldovich, Zh. Eksp. Teor. Fiz. **39**, 776 (1960) [Sov. Phys. JETP **39**, 542 (1960)].

[6] T. Vertse, K. F. Pál, and Z. Balogh, Comput. Phys. Commun. **27**, 309 (1982).

[7] M. Baldo, L. S. Ferreira, L. Streit, and T. Vertse, Phys. Rev. C **33**, 1587 (1986).

[8] L. Gr. Ixaru, M. Rizea, and T. Vertse, Comput. Phys. Commun. **85**, 217 (1995).

[9] R. Id Betan, R. J. Liotta, N. Sandulescu, and T. Vertse, Phys. Lett. B **584**, 48 (2004).

[10] R. I. Betan, A. T. Kruppa, and T. Vertse, Phys. Rev. C **78**, 044308 (2008).

[11] P. Salamon and T. Vertse, Phys. Rev. C **77**, 037302 (2008).

[12] T. Vertse, P. Curutchet, O. Civitarese, L. S. Ferreira, and R. J. Liotta, Phys. Rev. C **37**, 876 (1988).

[13] D. J. Millener, Nucl. Phys. A **693**, 394 (2001).

[14] N. Michel, W. Nazarewicz, M. Ploszajczak, and J. Okolowicz, Phys. Rev. C **67**, 054311 (2003).

[15] B. Gyarmati and T. Vertse, Nucl. Phys. A **160**, 523 (1971).

[16] E. I. Dolinsky and A. M. Mukhamedzhanov, Izv. AN. SSSR, Ser. Fiz. **41**, 2055 (1977) [Bull. Acad. Sci. USSR, Phys. Ser. **41**, 55 (1977)].

[17] A. Csótó and G. M. Hale, Phys. Rev. C **55**, 536 (1997).

[18] N. Michel1, W. Nazarewicz, M. Ploszajczak, and T. Vertse, J. Phys. G **36**, 013101 (2009).

[19] L. D. Blokhintsev, I. Borbely, and E. I. Dolinskii, Fiz. Elem. Chastits At. Yadra **8**, 1189 (1977) [Sov. J. Part. Nucl. **8**, 485 (1977)].

[20] A. M. Mukhamedzhanov and N. K. Timofeyuk, Pis'ma Zh. Eksp. Teor. Fiz. **51**, 247 (1990) [JETP Lett. **51**, 282 (1990)].

[21] H. M. Xu, C. A. Gagliardi, R. E. Tribble, A. M. Mukhamedzhanov, and N. K. Timofeyuk, Phys. Rev. Lett. **73**, 2027 (1994).

[22] A. M. Mukhamedzhanov, C. A. Gagliardi, and R. E. Tribble, Phys. Rev. C **63**, 024612 (2001).

[23] Yu. V. Orlov and B. F. Irgaziev, Izv. RAN, Ser. Fiz. **72**, 1625 (2008).

[24] L. P. Kok, Phys. Rev. Lett. **45**, 427 (1980).

[25] A. I. Baz', Ya. B. Zel'dovich, and A. M. Perelomov, *Scattering, Reactions and Decays in Nonrelativistic Quantum Mechanics* (Nauka, Moscow, 1971) [in Russian]; A. M. Perelomov and Ya. B. Zel'dovich, *Quantum Mechanics: Selected Topics* (World Scientific, Singapore, 1998).

[26] Albert Messiah, *Quantum Mechanics* (John Wiley & Sons, New York, 1966), Vol. I.

[27] R. G. Newton, *Scattering Theory of Waves and Particles* (McGraw-Hill, New York, 1966).

[28] A. M. Mukhamedzhanov *et al.*, Nucl. Phys. A **725**, 279 (2003).

[29] B. F. Irgaziev and Yu. V. Orlov, Izv. RAN, Ser. Fiz. **70**, 224 (2006).

[30] D. Baye, P. Descouvemont, and F. Leo, Phys. Rev. C **72**, 024309 (2005).

[31] C. Qi *et al.*, Int. J. Mod. Phys. E **17**, 1955 (2008).

[32] H. T. Fortune, Phys. Rev. C **74**, 054310 (2006).

[33] L. Canton, G. Pisent, J. P. Svenne, K. Amos, and S. Karataglidis, Phys. Rev. Lett. **96**, 072502 (2006).

[34] L. Canton *et al.*, Nucl. Phys. A **790**, 251c (2007).

[35] F. C. Barker, Phys. Rev. C **53**, 1449 (1996).

[36] F. C. Barker, Aust. J. Phys. **40**, 307 (1987).

[37] R. Sherr and G. Bertsch, Phys. Rev. C **32**, 1809 (1985).

[38] D. Y. Pang, F. M. Nunes, and A. M. Mukhamedzhanov, Phys. Rev. C **75**, 024601 (2007).

[39] G. Murillo, S. Sen, and S. E. Darden, Nucl. Phys. A **579**, 125 (1994).

[40] V. Z. Goldberg *et al.*, Phys. Rev. C **69**, 031302(R) (2004).

[41] F. Q. Guo *et al.*, Phys. Rev. C **72**, 034312 (2005).

[42] A. M. Lane and R. G. Thomas, Rev. Mod. Phys. **30**, 257 (1958).

[43] F. Ajzenberg-Selove, Nucl. Phys. A **506**, 1 (1990) [http://www.tunl.duke.edu/nucldata/chain/11_newv.shtml].

[44] D. J. Millener (private notes).

[45] D. Kurath and L. Picman, Nucl. Phys. **10**, 313 (1959).

[46] R. Sherr and H. T. Fortune, Phys. Rev. C **64**, 064307 (2001).

[47] V. Lima *et al.*, Nucl. Phys. A **795**, 1 (2007).

[48] A. M. Mukhamedzhanov *et al.*, Phys. Rev. C **56**, 1302 (1997).

[49] L. Axelsson *et al.*, Phys. Rev. C **54**, R1511 (1996).

[50] E. Casarejos *et al.*, Phys. Rev. C **73**, 014319 (2006).

[51] H. T. Fortune, D. Koltenuk, and C. K. Lau, Phys. Rev. C **51**, 3023 (1995).

[52] F. C. Barker, Phys. Rev. C **69**, 024310 (2004).

[53] G. B. Liu and H. T. Fortune, Phys. Rev. C **42**, 167 (1990).

[54] A. Lépine-Szily *et al.*, Phys. Rev. Lett. **80**, 1601 (1998).

[55] V. Guimaraes *et al.*, Phys. Rev. C **67**, 064601 (2003).

[56] K. Markenroth *et al.*, Phys. Rev. C **62**, 034308 (2000).

[57] P. Mohr, H. Beer, H. Oberhummer, and G. Staudt, Phys. Rev. C **58**, 932 (1998).

[58] G. E. Brown and A. D. Jackson, *The Nucleon-Nucleon Interaction* (North-Holland, Amsterdam, 1976).

[59] V. O. Yeremenko, L. I. Nikitina, and Yu. V. Orlov, Izv. RAN, Ser. Fiz. **71**, 819 (2007) [Bull. Russ. Acad. Sci.: Physics **71**, 791 (2007)].

[60] L. D. Blokhintsev, A. M. Mukhamedzhanov, and A. N. Safronov, Fiz. Elem. Chastits At. Yadra **15**, 1296 (1984) [Sov. J. Part. Nucl. **15**, 580 (1984)].

[61] Yu. V. Orlov and Yu. P. Orevkov, Yad. Fiz. **69**, 855 (2006) [Phys. At. Nucl. **69**, 828 (2006)].

[62] M. Abramowitz and I. A. Stegan, *Handbook of Mathematical Functions* (Dover, New York, 1968).

[63] [http://t2.lanl.gov/data/astro/molnix96/massd.html].